



A chirped-pulse Fourier-transform microwave/pulsed uniform flow spectrometer. I. The low-temperature flow system

James M. Oldham, Chamara Abeysekera, Baptiste Joalland, Lindsay N. Zack, Kirill Prozument, Ian R. Sims, G. Barratt Park, Robert W. Field, and Arthur G. Suits

Citation: *The Journal of Chemical Physics* **141**, 154202 (2014); doi: 10.1063/1.4897979

View online: <http://dx.doi.org/10.1063/1.4897979>

View Table of Contents: <http://scitation.aip.org/content/aip/journal/jcp/141/15?ver=pdfcov>

Published by the AIP Publishing

2014 Special Topics

- PEROVSKITES
- 2D MATERIALS
- MESOPOROUS MATERIALS
- BIOMATERIALS/ BIOELECTRONICS
- METAL-ORGANIC FRAMEWORK MATERIALS

AIP | APL Materials

Submit Today!

A chirped-pulse Fourier-transform microwave/pulsed uniform flow spectrometer. I. The low-temperature flow system

James M. Oldham,¹ Chamara Abeysekera,¹ Baptiste Joalland,¹ Lindsay N. Zack,¹ Kirill Prozument,¹ Ian R. Sims,² G. Barratt Park,³ Robert W. Field,³ and Arthur G. Suits^{1,a)}

¹Department of Chemistry, Wayne State University, 5101 Cass Avenue, Detroit, Michigan 48202, USA

²Institut de Physique de Rennes, UMR CNRS-UR1 6251, Université de Rennes 1, 263 Avenue du Général Leclerc, 35042 Rennes Cedex, France

³Department of Chemistry, Massachusetts Institute of Technology, Cambridge, Massachusetts 02139, USA

(Received 23 August 2014; accepted 30 September 2014; published online 20 October 2014)

We report the development of a new instrument that combines chirped-pulse microwave spectroscopy with a pulsed uniform supersonic flow. This combination promises a nearly universal detection method that can deliver isomer and conformer specific, quantitative detection and spectroscopic characterization of unstable reaction products and intermediates, product vibrational distributions, and molecular excited states. This first paper in a series of two presents a new pulsed-flow design, at the heart of which is a fast, high-throughput pulsed valve driven by a piezoelectric stack actuator. Uniform flows at temperatures as low as 20 K were readily achieved with only modest pumping requirements, as demonstrated by impact pressure measurements and pure rotational spectroscopy. The proposed technique will be suitable for application in diverse fields including fundamental studies in spectroscopy, kinetics, and reaction dynamics. © 2014 AIP Publishing LLC. [<http://dx.doi.org/10.1063/1.4897979>]

I. INTRODUCTION

The most sensitive and widely used detection methods in gas-phase physical chemistry studies (e.g., resonant photoionization, laser-induced fluorescence, mass spectrometry) often face serious challenges in relating signal intensities to actual concentrations of reaction products, and even relative quantities are seldom determined with confidence. Moreover, although powerful for revealing the dynamics of small systems,¹⁻³ these methods rarely provide detailed structural information. Traditional techniques face additional challenges in application to complex polyatomic systems where isomer-specific measurements may be key, although tunable synchrotron radiation has recently had a significant impact in this realm.⁴⁻⁶ Synchrotron beamtime is limited, however, and not widely accessible. Thus, a new technique is sought that will overcome these challenges and allow unimolecular and bimolecular reactions to be probed for large polyatomic systems such that branching ratios and vibrational distributions can be accurately determined, transient reaction intermediates characterized, and reaction kinetics measured with product identification and branching. To this end, we have developed a new instrument based on a uniform supersonic flow system⁷ combined with a chirped-pulse Fourier transform microwave (CP-FTMW) spectrometer.⁸⁻¹³ This chirped-pulse, uniform flow (CPUF) instrument can record ultra-broadband rotational spectra at MHz resolution for transient and *rotationally thermalized* reaction products. CP-FTMW is a very general spectroscopic method suitable for essentially any species that possesses at least a modest electric dipole moment. The subject of

the present article is to describe our new approach to the generation of cold pulsed uniform supersonic flows in a pulsed manner suitable for CP-FTMW, but readily adaptable to other detection methods as well.

Uniform supersonic flow systems have been developed and applied with great success for kinetics studies at low temperatures, as demonstrated by the CRESU technique (a French acronym for Reaction Kinetics in Uniform Supersonic Flows),^{7,14-16} and several subsequent instruments modeled after it.¹⁷⁻²¹ At the heart of these systems is a Laval nozzle, an axisymmetric convergent-divergent nozzle recognizable as the familiar rocket nozzle design, from which emerges a flow uniform in temperature, velocity, and density along the propagation axis. The density in these flows ($\sim 10^{16}-10^{17} \text{ cm}^{-3}$) is sufficiently high to offer the reactants and products a relatively dense, inert, and thermalized medium. The nozzle profile is typically optimized by a perturbative technique to solve the nonlinear, second-order Navier-Stokes equations of fluid motion, which describe the resultant flow pressure and temperature.¹⁴ Thus, Laval nozzles offer some advantages over the pulsed jet sources typically used in microwave spectrometers, namely: (1) they are equilibrium environments in which the temperature is stable throughout the flow; (2) reactive processes and photochemical systems can be cooled and thermalized uniformly; (3) the total number of sample molecules in the irradiated volume may be made quite large given high densities and large flow volumes, allowing greater signal levels.

Although continuous uniform supersonic flow systems offer an advantage over pulsed jet sources, there remain some disadvantages associated with them. A major drawback is that they consume vast quantities of gas and make extraordinary

^{a)} Author to whom correspondence should be addressed. Electronic mail: asuits@wayne.edu

demands on the pumping systems, rendering them too large and expensive for widespread use and precluding their use when expensive or scarce reactants are needed. To overcome these limitations, one could reduce the Laval nozzle dimensions, with the disadvantage of reducing the molecular cooling capabilities and reactant volumes,²² or pulse the uniform supersonic expansion, as pioneered by the Smith group at Arizona.^{17,23} Advantages of these pulsed systems have been demonstrated for many applications.^{18–20,24–27} One shortcoming of these designs, however, is that they have all been based on the use of solenoid actuated valves that deliver limited gas throughput. Because establishing a stable flow requires reaching stable target pressures upstream of the flow, typically ≥ 50 mbar in the stagnation region, small reservoir volumes have been employed and in some cases the valve is fired directly in the nozzle throat. Under these conditions, due to the minimal reservoir volume, the gas passes through the nozzle almost instantaneously and the valves may be held open for comparatively long times (> 10 ms) while a steady state builds throughout the setup. In part because the flow velocity prior to the convergent part of the nozzle is nonzero, the characteristics of the flow after the nozzle are altered. In particular, the flow temperature is higher than would be expected from a continuous flow with the same nozzle design. To date, pulsed uniform supersonic flow (PUSF) systems employing solenoid valves have not demonstrated flow temperatures below about 39 K,²⁸ with $T \sim 70$ – 90 K typically achieved. In an alternative approach developed recently, the reservoir is continuously filled, as it would be for a continuous nozzle, but the transmission of gas through the nozzle is pulsed by use of a high-speed spinning disk or chopper sealed in the divergent side of the Laval nozzle. Although this method reduces gas consumption and offers optimal flow conditions validated at 23 K,^{29,30} it is experimentally challenging to implement and results in only a reduction of a factor of 10 in gas consumption, thus it still requires substantial pumping.

CP-FTMW spectroscopy motivated the development of our new spectrometer because it allows for the acquisition of broadband spectra while providing near-universal detection and detailed structural characterization of molecular species. Because molecular rotational transitions have narrow linewidths (usually < 1 MHz) and are dependent principally on the moments of inertia, and because a single chirped microwave spectrum may contain 10^4 or 10^5 resolution elements, unambiguous identification of a specific molecule can be made even in a congested spectrum with several different species or isomers present. Moreover, the intensities of the spectral lines are reliable indicators of relative species' populations, making it possible to accurately determine branching ratios and, in some cases, vibrational distributions.³¹ Thus, when combined with a PUSF source, this combined CPWF technique is uniquely well-suited for studying polyatomic unimolecular and bimolecular reaction dynamics and kinetics.

We present here a new approach to generate pulsed uniform supersonic flows with temperatures as low as 20 K. This method, relying on use of a high-throughput piezoelectric stack valve, offers increased ease of use and flexibility, while reducing the gas load and demands of the pumping system to 0.5%–5% relative to the continuous case. The effective-

ness of this technique is demonstrated through impact pressure measurements and spectroscopic characterization. These data confirm that a high-density, uniform flow with temperatures and densities around 20–30 K and 10^{16} cm⁻³, respectively, is achieved in both argon and helium carrier gases.

II. EXPERIMENTAL

The aim of this experiment is to take the well-proven technique of uniform supersonic Laval flows in chemical kinetics and adapt it to achieve flow temperatures on the order of 20 K in a form that is economical and convenient to construct and operate, and is optimized for coupling to the chirped pulse microwave spectrometer. In Sec. II A, the considerations that guided our experimental design are discussed, followed by a description of the apparatus that satisfies these considerations in Sec. II B.

A. Design considerations

Laval flows suitable for dynamics and kinetics studies typically employ pressures on the order of 40–80 mbar in the stagnation region and 0.1–0.6 mbar in the flow region. For example, a typical continuous flow of 35 SLM (standard dm³ min⁻¹) at a pressure of 0.4 mbar in the flow chamber requires a pumping speed of more than 20 000 l s⁻¹. This volume flow rate requirement places enormous demands on the pumping systems, thus the typical continuous flow systems employed in kinetics studies use large Roots blowers to handle this gas load. For our purposes, a system operating at 2–10 Hz is acceptable if a stable flow on the order of 1 ms duration can be established. For a 2 ms pulse at 10 Hz, we reduce the volume throughput of the prototype argon flow discussed above to 0.7 SLM. Although this pressure regime (0.1–0.6 mbar) is well-matched to Roots blowers, they have undesirable qualities such as noise, vibration, and a need for regular maintenance. Modern compound turbomolecular pumps based on magnetic levitation present an appealing alternative. They can readily achieve the target volume flow rates at these pressures, as well as being silent and essentially maintenance-free. We have thus chosen a high-throughput compound turbomolecular pump as the primary pumping stage for the flow. In our designs, the stability of pressure conditions over several cycles was also considered. A one-dimensional model of the flow conditions through the chamber suggested that there is rapid convergence to steady-state pressure conditions in the flow chamber, and complete evacuation of the chamber between pulses is unnecessary.

Improvement of the pulsed flow conditions to match the low temperatures obtained by continuous flows suggests two significant changes to the reservoir loading scheme from those used in other pulsed Laval systems. First, a reservoir volume of ~ 15 cm³ is chosen to ensure a negligible mean reservoir gas velocity prior to entry into the nozzle. Also, the flow characteristics of the gas through the nozzle must closely approximate those calculated for a specific nozzle design. Second, the reservoir must be capable of rapid loading, with the reservoir pressure above that for optimal uniform flow immediately

after the loading ends. This rapid loading is deemed necessary since there is no barrier to flow through the nozzle, which results in flow beginning as soon as a positive pressure difference occurs between the reservoir and the flow chamber. Rapid loading thus minimizes the consumption of gas that would otherwise be wasted while the reservoir pressure is brought up to the desired value. Slow loading also leads to greater total gas consumption, because much longer pulses are then required. In ideal circumstances, loading should be complete within a few hundred microseconds, which demands a flow rate through the valve that must for a brief period greatly exceed the continuous flow requirement of 35 SLM. This flow rate is larger than what is typically possible with a conventional solenoid valve. Therefore, a piezoelectric stack valve inspired by the work of the Gentry group,³² which combines high forces and linear displacement, was designed to meet this requirement.

B. Experimental setup

A schematic diagram of the experimental apparatus, which satisfies the considerations and restrictions discussed above, is shown in Fig. 1, and is briefly described here prior to a more detailed description below of each of the individual components. The new design of the pulsed valve, driven by a piezoelectric stack actuator, repetitively fills the reservoir upstream from the Laval nozzle. Two Laval nozzles, designed for uniform flows of different flow velocities and carrier gases (helium and argon), have been implemented. The carrier gas flows out of the nozzle into the reaction chamber, a cylindrical polycarbonate tube with a volume of 50 l, that is transparent to visible and microwave radiation. Microwave antennae on opposite sides of the chamber transmit and receive microwave radiation, as described fully in a following paper. The chamber is mounted on a home-built translation stage so that its movement along the propagation axis will

permit interrogation of the flow at various downstream distances from the nozzle while keeping the antenna positions fixed. Two fast pressure transducers, one located in the reservoir and the other mounted in a Pitot tube downstream of the nozzle, are used to monitor flow pressures so that the required conditions are achieved. Aluminum flanges are mounted on each end of the polycarbonate tube and sealed with o-rings. A turbomolecular pump coupled to a dual stage rotary pump is connected to the downstream end of the chamber.

A schematic of the nozzle assembly is shown in Fig. 2. Valves based upon piezoelectric transducers were developed in the early 1980s as molecular beam sources. The initial designs evolved through contributions from several groups^{33,34} and a commercial model was developed, all based upon disk translators. An optimal design published by Proch and Trickl has seen very wide use.³⁵ These have the advantage of very fast opening times and translational motion of 100 μm or more. However, these disk translators have a maximum pulling force of only 10 N, which limits their ability to open large nozzles at high pressure quickly enough to achieve the gas throughput requirements needed here. Our valve instead employs a high force piezoelectric stack actuator (Physik Instrumente, P-212.80). This actuator can achieve up to 120 μm linear motion of the plunger with 2000 N pushing and 300 N pulling, 15 times greater than the disk translators. As a result, large nozzles can easily be opened quickly against very high backing pressures, and the piezo stack can readily be isolated from the gas itself.

The plunger is composed of a 4 mm diameter, 2.5 cm long cylinder that is directly screwed onto the actuator; a groove is cut at the end of the plunger for a Kalrez o-ring that seals off the 5 cm^3 stagnation volume of the valve from the reservoir. Alternatively, a T-shaped plunger can be used to seal off the nozzle on the outer side of the front plate, thus operating in a normally-closed mode, as these actuators are extended when a potential is applied. We have

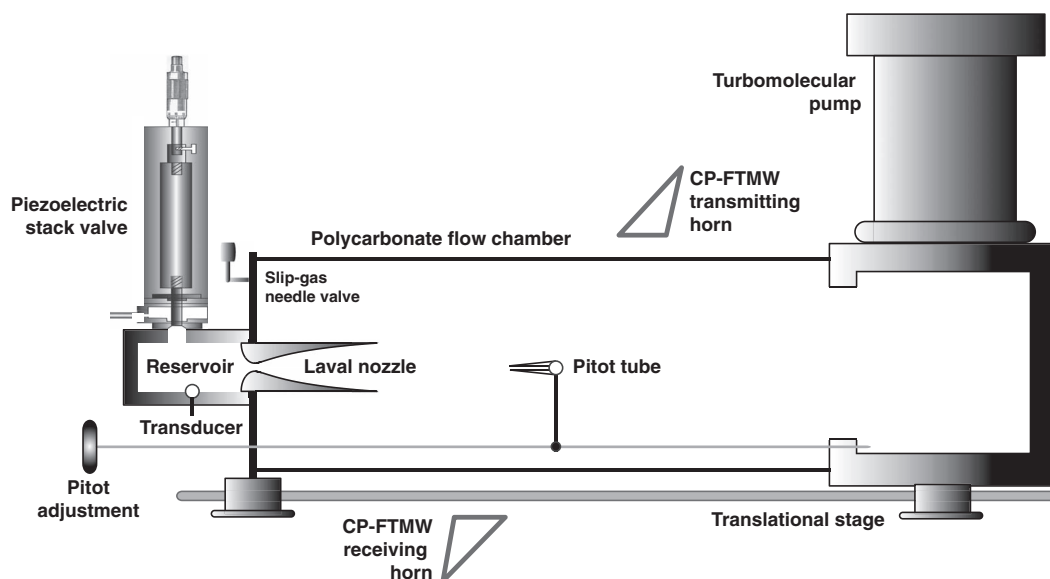


FIG. 1. The pulsed uniform supersonic flow system. The stacked piezoelectric valve is mounted on a reservoir outside of the vacuum chamber. Pressures in the reservoir and main chambers are monitored by pressure transducers mounted on the reservoir and inside of a Pitot tube, respectively. The vacuum chamber consists of a polycarbonate tube of outside diameter ~ 30 cm which is transparent in the microwave spectral region. The figure is not to scale.

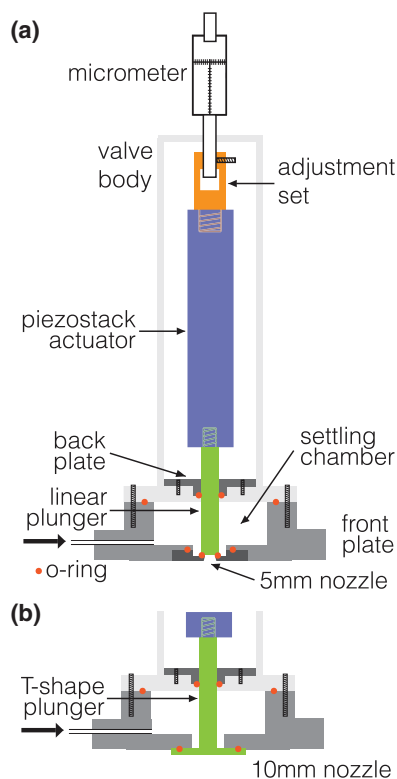


FIG. 2. Cut-away view of the valve assembly. The piezostack actuator (blue) is mounted in a stainless steel valve body (light grey). The position of the plunger (green), either linear (a) or T-shaped (b), is adjusted by a micrometer. The different o-ring positions are symbolized by red circles. In particular, the plunger is sealed at two positions, i.e., by an o-ring at the nozzle itself, and by another o-ring fixed at the top of the plunger with its tightness adjusted by varying the pressure exerted by the back plate.

successfully tested both approaches, although we present here only the results obtained with a linear plunger in a normally-open configuration. A micrometer head (Mitutoyo 110-102) allows for fine adjustment of the actuator and plunger to maximize the gas flow. The valve is mounted vertically onto a 15 cm³ cylindrical reservoir, which serves as a settling region prior to flow through the nozzle. When the valve is fully open, gas flows into the reservoir through a cross-section of ~ 1.5 mm². The valve is closed by applying a constant high voltage (+800 V) from a HV power supply. The applied voltage is rapidly grounded by a HV fast switch (Behlke HTS-61-03-GSM), which causes the piezoelectric material to contract, thereby opening the valve. The voltage is rapidly switched on again to reclose the valve. Repetition rates of 2 to 10 Hz and pulse widths with various durations are controlled by a pulse delay generator (Berkeley Nucleonics Corporation 575-8 C).

The PUSF system can accommodate one of two in-house machined Laval nozzles that are designed to produce uniform

supersonic flows, one for a uniform argon flow, the other for a uniform helium flow. Mach numbers of 5.47 from the argon nozzle and 5.45 from the helium nozzle are achieved. The nozzles are machined from aluminum alloy 2024 with an outer diameter of 74 mm. The throat and exit diameters are, respectively, 8 and 55 mm for the argon nozzle and 3 and 20 mm for the helium nozzle. The design pressures for the reservoir (P_0) and the flow chamber (P_f), as well as the other design profile parameters, are shown in Table I.

The pumping scheme consists of an 1100 l s⁻¹ (N₂) compound turbomolecular pump (Osaka Vacuum, TG1113MBW-90) backed by a 20 l s⁻¹ (N₂) rotary pump (Edwards E2M80). This combination can maintain an operating pressure in the chamber up to 0.6 mbar while the valve is in operation, with repetition rates of 1–10 Hz, and an unloaded pressure on the order of 10⁻⁶ mbar. The pressure inside the chamber is monitored using a calibrated pressure transducer (MKS Baratron), mounted at the end of the chamber. The flow conditions are monitored by two pressure transducers (Kulite XCEL-100-5A). One transducer is mounted on the reservoir wall and the other inside a Pitot tube, which can be longitudinally and radially adjusted along the flow propagation axis with a rotary-linear motion feedthrough (MDC vacuum). The outputs of the two sensors are amplified by a signal conditioner (Endevco model 126) and monitored on a 100 MHz oscilloscope (Tektronix DPO2014B). After calibration of the transducers with the Baratron pressure gauge located inside the flow chamber, the flow duration, temperature profile, Mach number, and density along the flow axis can be determined (see Sec. III).

Several steps are taken in order to ensure the uniformity of the flow. By overpressuring the stagnation chamber, for example, it is possible to obtain a uniform flow at a designated temperature range for times up to 200–500 μ s, depending on the flow gas. This method also reduces flow turbulence, a common problem in other pulsed Laval systems. Equalizing pressure in the chamber can minimize boundary layer formation, either by varying the repetition rate of the gas pulse or by loading a slip gas directly into the chamber through a needle valve.

III. RESULTS

The performance of both the helium and argon nozzles was characterized by impact pressure measurements (Sec. III A). In doing so, 2D profiles of the flow temperatures and densities were obtained to estimate the isentropic core and boundary layer dimensions. Additionally, the temperature of the helium flow was independently determined via a Boltzmann analysis using the integrated line intensities of several

TABLE I. Mach numbers, M , target pressures, P_0 and P_f , temperatures, T , and densities, n , of the uniform flows estimated by the flow simulations for the Ar and He Laval nozzles. T_m and n_m are the corresponding values deduced from the impact pressure measurements.

M	Gas	P_0 (mbar)	P_f (mbar)	T (K)	n (10 ¹⁶ molecule cm ⁻³)	T_m (K)	n_m (10 ¹⁶ molecule cm ⁻³)	Uniform distance (cm)
5.47	Ar	76.5	0.190	26.6	5.23	26 \pm 1	4.84	20
5.45	He	69.4	0.183	27.0	4.72	22 \pm 2	3.78	10

pure rotational transitions of dimethyl ether, CH_3OCH_3 , and acetaldehyde, CH_3CHO (Sec. III B).

A. Impact pressure measurements

The profiles of the flows of the Ar and He Laval nozzles, based on the impact pressure measurements, are shown in Fig. 3. The impact pressures were recorded along the flow axis with the Pitot tube initially oriented such that the pressure transducer was located at the nozzle exit, and then in 1 cm downstream increments. In the Ar profile (Fig. 3(a)), the flow is very stable and uniform out to distances of almost 20 cm from the nozzle exit. The impact pressure shows negligible fluctuations over a duration of about 4 ms shortly after the valve opening, staying at ~ 7 mbar. Further evidence that the flow is well collimated and uniform is given by the radial distributions shown at linear distances 0, 8, and 16 cm in Fig. 3(b). In the He profile (Fig. 3(c)), the impact pressure fluctuates from the nozzle exit to a linear distance of around 12 cm, and then begins to decrease. Nonetheless, through the core, the impact pressure remains relatively constant at around 7 mbar. The radial profiles of the helium flow at 0, 4, 8, and 10 cm from the nozzle exit (Fig. 3(d)) are similar to each other, although they reach maximum values at increasingly lower impact pressures, reflecting the tapered profile in Fig. 3(c). These curves do not display the pronounced “flat-top” appearance of the argon radial distribution, and the decrease in impact pressure relative to radial distance seems more gradual. These differences can be attributed to the much smaller inner diameter of the He nozzle.

One feature of the pulsed Laval technique that differentiates it from other pulsed supersonic expansion methods is its temperature stability along the propagation axis. Assuming that the flow is isentropic, the Mach number M can be

estimated from the Rayleigh formula:

$$\frac{P_i}{P_0} = \left[\frac{(\gamma + 1)M^2}{(\gamma - 1)M^2 + 2} \right]^{\frac{\gamma}{(\gamma-1)}} \left[\frac{(\gamma + 1)}{(2\gamma M^2 - \gamma + 1)} \right]^{\frac{1}{(\gamma-1)}}, \quad (1)$$

where P_0 and P_i are, respectively, the reservoir pressure and the impact pressure, and $\gamma = C_p/C_v$ is the ratio of specific heat capacities. With a stagnation chamber held at room temperature, the flow temperature (T_f) and pressure (P_f) are then calculated via

$$\frac{T_0}{T_f} = 1 + \frac{\gamma - 1}{2} M^2 \quad (2)$$

and

$$\frac{P_0}{P_f} = \left(\frac{T_0}{T_f} \right)^{\frac{\gamma}{(1-\gamma)}}. \quad (3)$$

Hence, the Mach number measurements using the isentropic hypothesis allow verification that the experimental flow conditions are in good agreement with the predicted ones, i.e., when a consistent match is achieved for the flow and static chamber pressures. *Once these conditions are reached, one can determine the temperature, pressure, and density at any point of the flow.*

The temperature profiles of the argon and helium beams determined by this method are presented in Fig. 4. For Ar, the temperature shows little variation out to 18 cm, with an average value of $T = 26 \pm 1$ K. For He, the fluctuations observed in Fig. 3 are also apparent, but still are quite modest: although the temperature at the nozzle reaches a maximum of ~ 24 K, the temperature stabilizes to ~ 22 K at a distance of 2 cm from the nozzle exit. Notably, at distances between 3 and 7 cm, where the uniform flow is typically probed by the microwave spectrometer, there is less than a ± 1 K variation

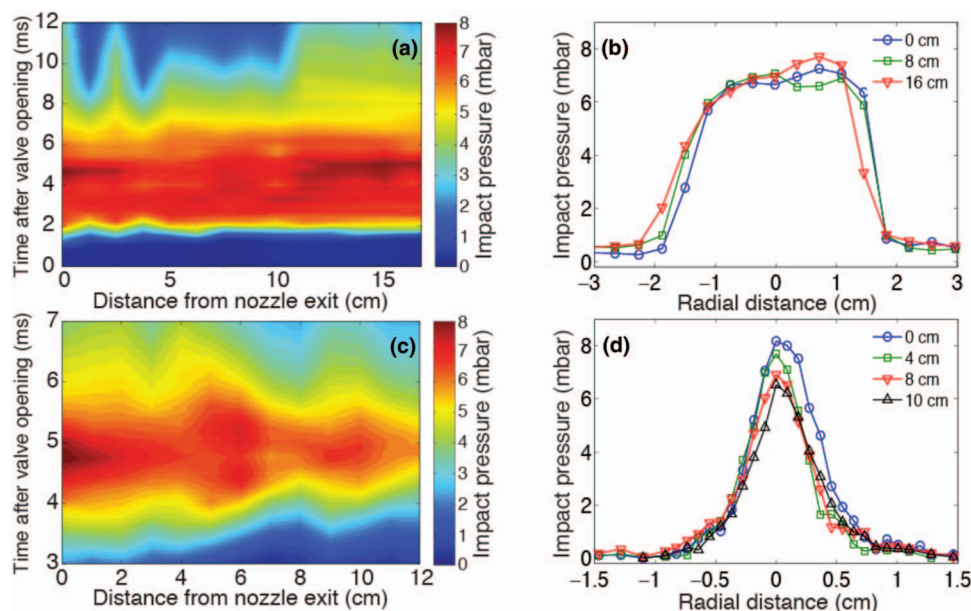


FIG. 3. (a) and (c) The impact pressure profiles of Ar and He Laval nozzles, with exit diameters of 55 and 20 mm, respectively, are shown for times up to 12 and 7 ms after the valve is opened, with uniform flow maximum distances of 17 and 12 cm, respectively. (b) and (d) Radial profiles of the Ar and He flows for several distances between 0 and 16 cm and 0 and 10 cm, respectively, with nearly uniform isentropic core diameters of ~ 3 and ~ 1 cm, respectively ($P_i > 7$ mbar).

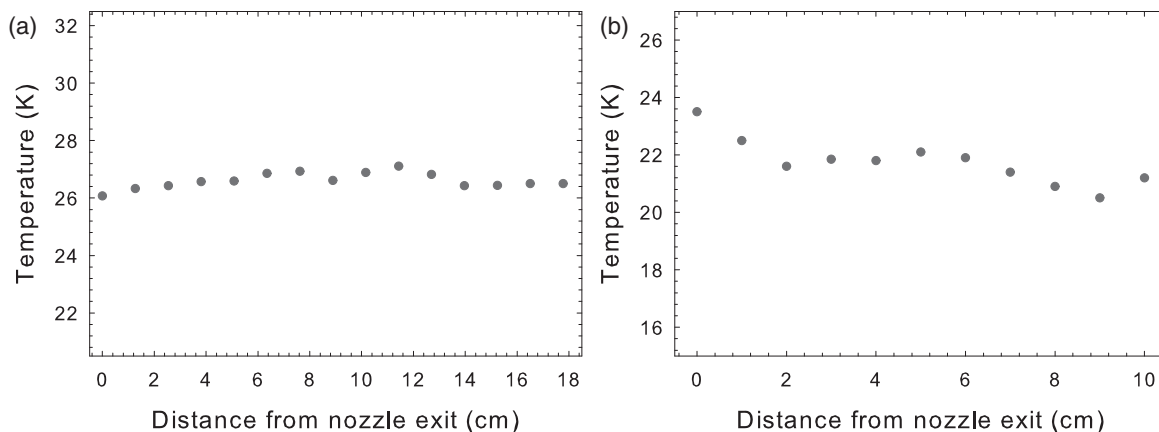


FIG. 4. (a) The argon flow temperature calculated from Pitot tube pressure measurements measured at different linear distances. The temperature ($T = 27 \pm 1$ K) shows very little variation out to distances of 18 cm. (b) Pitot measurements of the helium flow indicate a temperature of around $T = 22 \pm 2$ K for distances out to 10 cm. The initial temperature “spike” ($T = 23.5$ K) at the nozzle exit may be due to turbulence. At distances between 3 and 6 cm, where the microwave transmitting and receiving horns are usually located, the variation in temperature is < 1 K.

in temperature. Beyond 10 cm (not shown), a significant and rapid decrease of the impact pressure is observed. The temperatures and densities obtained from these measurements are given in Table I, and show excellent agreement with the design parameters of both nozzles.

B. Rotational temperature

We note that the impact pressure analysis above assumes that the gas in the reservoir is at room temperature. That this is a valid assumption despite the initial expansion into the chamber is demonstrated in the rotational spectra for the helium case in the following paragraphs. We have not been able to obtain similar spectra in argon and there are several possible reasons for this. Clustering in argon is a much greater problem than in helium owing to a “chaperone” effect involving dimers. In addition, argon has a much lower thermal conductivity, so that the cooling that accompanies the initial expansion may persist. In this case our impact pressure measurement might significantly overestimate the flow temperature for argon. We plan future experiments with a temperature-variable reservoir to investigate this.

The pure rotational spectra of dimethyl ether, CH_3OCH_3 , and acetaldehyde, CH_3CHO , were recorded over the 34–40 GHz range and used to assess the rotational temperature of the helium flow using a Boltzmann analysis. Both molecules are closed-shell asymmetric tops containing either one or two methyl rotors, which cause each $J'(K_a', K_c') - J''(K_a'', K_c'')$ rotational transition to split into multiple components. For acetaldehyde, the methyl rotation results in fully-resolvable doublets, denoted A and E. Thus, the analysis for acetaldehyde was based on 12 distinct spectral lines. Dimethyl ether, however, contains two methyl rotors, which produce quartets of blended or partially-blended lines (AA, EE, AE, and EA). Therefore, although 15 spectral features due to CH_3OCH_3 were recorded, lines belonging to the same $J'(K_a', K_c') - J''(K_a'', K_c'')$ transition were collapsed and the center frequency taken as the average frequency of the quartet and the total line intensity as the sum of the individual intensities.

The Boltzmann plots were constructed using the following relationship between the integrated line intensities (W) and corresponding lower state energies (E_l):³⁶

$$W = \frac{4\pi^{3/2}\omega_0^2 S \mu_i^2 g_i g_l \varepsilon}{c\sqrt{\alpha}} \frac{N_{\text{tot}}}{kT Q_{\text{rot}}} e^{-E_l/kT_{\text{rot}}}, \quad (4)$$

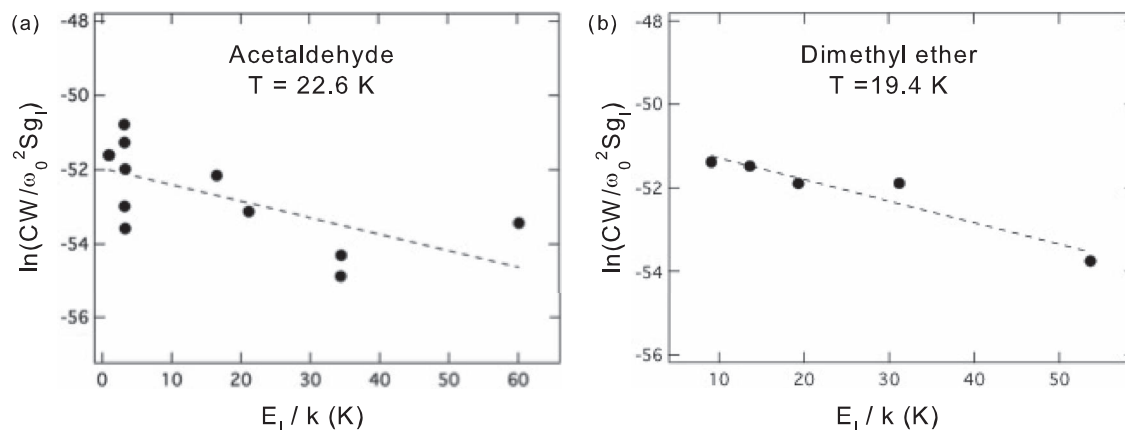


FIG. 5. Boltzmann plots for acetaldehyde (a) and dimethyl ether (b) in the helium flow. A linear least squares regression (1σ) yields rotational temperatures of $T_{\text{rot}} = 22.6 \pm 7$ and 19.4 ± 3 K, respectively. To simplify the y-axis label, C is used to represent the constants in Eq. (4).

with k the Boltzmann constant, ω_0 the transition frequency, α the sweep rate and N_{tot} , Q_{rot} , and T_{rot} the column density, partition function, and rotational temperature, respectively. The quantities S , μ_i , and g_i represent the line strength, dipole moment, and nuclear spin weight. If the logarithm of both sides of Eq. (4) is taken and the expression rearranged, then a plot of $\ln(c\sqrt{\alpha} W/4\pi^3 \omega_0^2 S \mu_i^2 g_i g_e \epsilon)$ vs. E_i/k yields a line, the slope of which is the inverse of the rotational temperature, with an intercept of $\ln(N_{\text{tot}}/kTQ_{\text{rot}})$.

Figure 5 shows Boltzmann plots of CH_3CHO and CH_3OCH_3 , based on spectra measured ~ 4 cm downstream from the nozzle exit. The integrated line intensities were taken as the areas of the peaks, as determined from the Igor Pro (WaveMetrics, Inc., Lake Oswego, OR, USA) multipeak fitting package. The values for S , μ_i , and g_i were taken from the literature.^{37,35} From the least-squares fit of these data, temperatures of 19.4 ± 3 and 22.6 ± 7 K were derived for acetaldehyde and dimethyl ether, respectively, in good agreement with the impact pressure measurements.

IV. CONCLUSIONS

The objective of the presented pulsed uniform supersonic flow system was to obtain a collimated, high-density molecular flow at constant temperatures approaching 20 K and with hydrodynamic times of several hundreds of microseconds. We have demonstrated here, both by impact pressure and spectroscopic measurements, that these goals were achieved by using a dedicated high-throughput valve based on a piezoelectric stack actuator with only moderate pumping requirements. This design provides a versatile approach well suited for use with any detection technique. In the second article of this series of two, we will show that this new flow chamber allows for chemical dynamics studies of photolytic and bimolecular reactions by combining pulsed uniform supersonic expansion with the revolutionary CP-FTMW spectroscopic technique.

ACKNOWLEDGMENTS

This work was supported by the National Science Foundation (NSF), Award MRI-ID 1126380. I.R.S. thanks the CNRS and the Université de Rennes 1 for funding to support this collaboration. A.G.S. gratefully acknowledges an A. Paul and Carol Schaap Senior Faculty Fellowship and the Radboud Excellence Initiative. We also acknowledge valuable discussions with John Muentner and Brooks Pate.

¹D. Townsend, W. Li, S. K. Lee, R. L. Gross, and A. G. Suits, *J. Phys. Chem. A* **109**(39), 8661–8674 (2005).

²P. Casavecchia, *Rep. Prog. Phys.* **63**(3), 355–414 (2000).

³Y. T. Lee, *Science* **236**, 793 (1987).

- ⁴T. A. Cool, K. Nakajima, T. A. Mostefaoui, F. Qi, A. McIlroy, P. R. Westmoreland, M. E. Law, L. Poisson, D. S. Peterka, and M. Ahmed, *J. Chem. Phys.* **119**(16), 8356–8365 (2003).
- ⁵C. A. Taatjes, N. Hansen, A. McIlroy, J. A. Miller, J. P. Senosiain, S. J. Klippenstein, F. Qi, L. Sheng, Y. Zhang, and T. A. Cool, *Science* **308**(5730), 1887–1889 (2005).
- ⁶C. A. Taatjes, N. Hansen, D. L. Osborn, K. Kohse-Hoinghaus, T. A. Cool, and P. R. Westmoreland, *Phys. Chem. Chem. Phys.* **10**(1), 20–34 (2008).
- ⁷I. R. Sims, J.-L. Queffelec, A. Defrance, C. Rebrion-Rowe, D. Travers, P. Bocherel, B. R. Rowe, and I. W. M. Smith, *J. Chem. Phys.* **100**, 4229 (1994).
- ⁸G. G. Brown, B. C. Dian, K. O. Douglass, S. M. Geyer, S. T. Shipman, and B. H. Pate, *Rev. Sci. Instrum.* **79**(5), 053103 (2008).
- ⁹D. P. Zaleski, J. L. Neill, M. T. Muckle, N. A. Seifert, P. Brandon Carroll, S. L. Widicus Weaver, and B. H. Pate, *J. Mol. Spectrosc.* **280**, 68–76 (2012).
- ¹⁰B. C. Dian, G. G. Brown, K. O. Douglass, and B. H. Pate, *Science* **320**(5878), 924–928 (2008).
- ¹¹G. B. Park, A. H. Steeves, K. Kuyanov-Prozument, J. L. Neill, and R. W. Field, *J. Chem. Phys.* **135**(2), 024202 (2011).
- ¹²J. L. Neill, K. O. Douglass, B. H. Pate, and D. W. Pratt, *Phys. Chem. Chem. Phys.* **13**(16), 7253–7262 (2011).
- ¹³R. G. Bird, J. L. Neill, V. J. Alstadt, J. W. Young, B. H. Pate, and D. W. Pratt, *J. Phys. Chem. A* **115**(34), 9392–9398 (2011).
- ¹⁴G. Dupeyrat, J. B. Marquette, and B. R. Rowe, *Phys. Fluids* **28**, 1273–1279 (1985).
- ¹⁵I. Sims, J.-L. Queffelec, A. Defrance, C. Rebrion-Rowe, D. Travers, B. R. Rowe, and I. Smith, *J. Chem. Phys.* **97**, 8798–8800 (1992).
- ¹⁶I. R. Sims, J.-L. Queffelec, D. Travers, B. R. Rowe, L. B. Herbert, J. Karthäuser, and I. W. Smith, *Chem. Phys. Lett.* **211**, 461–468 (1993).
- ¹⁷D. B. Atkinson and M. A. Smith, *Rev. Sci. Instrum.* **66**, 4434 (1995).
- ¹⁸T. Van Marter and M. C. Heaven, *J. Chem. Phys.* **109**, 9266–9271 (1998).
- ¹⁹S. Lee, R. J. Hoobler, and S. R. Leone, *Rev. Sci. Instrum.* **71**, 1816–1823 (2000).
- ²⁰T. Spangenberg, S. Köhler, B. Hansmann, U. Wachsmuth, B. Abel, and M. A. Smith, *J. Phys. Chem. A* **108**, 7527–7534 (2004).
- ²¹N. Daugey, P. Caubet, B. Retail, M. Costes, A. Bergeat, and G. Dorthe, *Phys. Chem. Chem. Phys.* **7**(15), 2921–2927 (2005).
- ²²J. Daranlot, M. Jorfi, C. Xie, A. Bergeat, M. Costes, P. Caubet, D. Xie, H. Guo, P. Honvault, and K. M. Hickson, *Science* **334**, 1538–1541 (2011).
- ²³D. B. Atkinson and M. A. Smith, *J. Phys. Chem.* **98**, 5797–5800 (1994).
- ²⁴S. Lee and S. R. Leone, *Chem. Phys. Lett.* **329**, 443–449 (2000).
- ²⁵T. P. Marcy, R. R. Díaz, D. Heard, S. R. Leone, L. B. Harding, and S. J. Klippenstein, *J. Phys. Chem. A* **105**, 8361–8369 (2001).
- ²⁶T. van Marter, M. C. Heaven, and D. Plummer, *Chem. Phys. Lett.* **260**, 201–207 (1996).
- ²⁷B. Hansmann and B. Abel, *ChemPhysChem* **8**, 343–356 (2007).
- ²⁸R. Sánchez-González, R. Srinivasan, J. Hofferth, D. Y. Kim, A. J. Tindall, R. D. W. Bowersox, and S. W. North, *AIAA J.* **50**(3), 691–697 (2012).
- ²⁹S. B. Morales, Ph.D. thesis, Université Rennes 1, 2009.
- ³⁰S. Cheikh Sid Ely, S. B. Morales, J.-C. Guillemin, S. J. Klippenstein, and I. R. Sims, *J. Phys. Chem. A* **117**(46), 12155–12164 (2013).
- ³¹K. Prozument, G. B. Park, R. G. Shaver, A. K. Vasiliou, J. M. Oldham, D. E. David, J. S. Muentner, J. F. Stanton, A. G. Suits, G. B. Ellison, and R. W. Field, *Phys. Chem. Chem. Phys.* **16**, 15739–15751 (2014).
- ³²F. Luo, Ph.D. thesis, University of Minnesota, 1995.
- ³³A. Auerbach and R. Mediarid, *Rev. Sci. Instrum.* **51**(9), 1273–1275 (1980).
- ³⁴J. B. Cross and J. J. Valentini, *Rev. Sci. Instrum.* **53**(1), 38–42 (1982).
- ³⁵D. Proch and T. Trickl, *Rev. Sci. Instrum.* **60**(4), 713–716 (1989).
- ³⁶C. H. Townes and A. L. Schawlow, *Microwave Spectroscopy* (Dover Publications, 1955).
- ³⁷F. J. Lovas, H. Lutz, and H. Dreizler, *J. Phys. Chem. Ref. Data* **8**, 1051–1107 (1979).